

# Pattern recognition using spiking antiferromagnetic neurons

Hannah Bradley<sup>1</sup>, Steven Louis<sup>2</sup>, Andrei Slavin<sup>1</sup>, and Vasyl Tyberkevych<sup>1</sup>

<sup>1</sup>*Department of Physics, Oakland University, Rochester MI 48309*

<sup>2</sup>*Department of Electrical Engineering, Oakland University, Rochester MI 48309*

## Abstract

Spintronic devices offer a promising avenue for the development of nanoscale, energy-efficient artificial neurons for neuromorphic computing. It has previously been shown that with antiferromagnetic (AFM) oscillators, ultra-fast spiking artificial neurons can be made that mimic many unique features of biological neurons. In this work, we train an artificial neural network of AFM neurons to perform pattern recognition. A simple machine learning algorithm called spike pattern association neuron (SPAN), which relies on the temporal position of neuron spikes, is used during training. In under a microsecond of physical time, the AFM neural network is trained to recognize symbols composed from a grid by producing a spike within a specified time window. We further achieve multi-symbol recognition with the addition of an output layer to suppress undesirable spikes. Through the utilization of AFM neurons and the SPAN algorithm, we create a neural network capable of high-accuracy recognition with overall power consumption on the order of picojoules.

## Introduction

Despite the increase in the computational capability of typical von Neumann architecture, the human brain still outperforms modern computers at classification tasks with a fraction of power consumption. By mimicking brain-like behaviors through hardware-implemented artificial neural networks, neuromorphic chips perform pattern recognition with reduced power consumption and increased efficiency.

A biological neural network is comprised of two critical components: the individual processing units called neurons and the synapses that determine their connections. Current neuromorphic chips use silicon-based transistors to make up both of these components [1]. In spite of the fact that transistor-based neuromorphic computing is an improvement over von Neumann architecture, a number of drawbacks still exist. Mainly, it requires multiple transistors to create one artificial neuron, thereby requiring a large amount of physical area and increasing power consumption.

In recent years, there has been growing interest in the use of spintronic devices for neuromorphic computing [2], [3]. Spintronic artificial neurons offer numerous advantages over their transistor-based counterparts. Apart from possessing intrinsic non-linear dynamics, these neurons can be fabricated at the nanoscale, with each device serving as a single neuron. As a result, power and area requirements are significantly reduced. The creation of artificial neurons has been shown to be possible with domain wall motion [4]–[6], skyrmions [7]–[9], spin torque nano oscillators [10]–[12], and magnetic tunnel junctions [13], [14].

One of the prospective designs of artificial spintronic neurons is based on antiferromagnetic (AFM) spin-Hall oscillators operating in a subcritical regime [15]. The main advantages of artificial AFM neurons are their nano-sized footprint, relatively low power consumption, and ultra-high operational [16]. In addition, AFM neurons feature many properties closely resembling biological neurons, such as bursting and refraction time. With constant coupling synapses, AFM neurons can create simple neural networks such as inhibitors and memory loops

[16]. These constant synapses can be realized in hardware by a copper bridge that would carry spikes from neuron to neuron.

An important question in spintronic neuromorphic research is whether more complex neural networks based on AFM neurons can be trained for cognitive tasks like pattern recognition and how efficient these networks are in terms of training and recognition time and power consumption. To a large extent, this problem depends on the efficient implementation of *variable* spintronic synapses capable of changing inter-neuron connectivity. This need for variable synapses dramatically increases the complexity of a neural network. This problem is even more serious for AFM neurons since, to fully employ ultra-fast AFM dynamics in neuromorphic hardware, reaction times of artificial synapses should be on a timescale of AFM neuron dynamics.

A less demanding approach is based on the idea of reservoir computing, which only trains synapses connected to the output layer [17], reducing the number of variable synapses needed and simplifying the overall neural network. Several simple learning algorithms are known for reservoir computing. In particular, a supervised learning algorithm called spike pattern association neuron (SPAN) limits the number of output neurons to one, simplifying the neural network even more [18]. The meaningful recognition tasks are possible in the SPAN algorithms by employing temporal encoding and matching outgoing spikes to a desired time.

In this work, we theoretically investigate the possibility of using AFM neurons combined with the SPAN algorithm to create neural networks that recognize symbols generated from a grid of input neurons. We show that, due to the strongly nonlinear and inertial dynamics of AFM neurons, even a single AFM neuron is capable of successfully recognizing various symbols from a  $5 \times 5$  input grid, which is enough to encode various printed symbols. Our simulations show that the total training time of AFM SPAN neuron can be below  $1 \mu\text{s}$  while the power consumption during the training is of the order of 30 pJs. This proves the potential of using artificial AFM neurons in time- and power-critical applications.

## Methods

Antiferromagnets (AFM) have two magnetic sublattices orientated in opposing directions. The direction of AFM magnetic sublattices relative to the crystal lattice can be manipulated using spin currents. Usually, this is achieved in spin Hall geometry, in which a layer of heavy metal covers an AFM element. When a DC electric current flows in the heavy metal layer, it induces a perpendicular spin current that penetrates into the AFM.

The most interesting effect of spin current on the AFM dynamics happens when the spin polarization of the spin current is perpendicular to the easy plane of the AFM. In this case, spin-transfer torque induced by a sufficiently large spin current causes the AFM sublattices to rotate in the easy plane [19]. For AFM materials with bi-axial anisotropy, the rotation of the sublattices is not uniform with time. This results in a sequence of short spin-pumping spikes at a frequency that can reach the THz range. The threshold current needed to achieve this auto-oscillating

regime depends on the easy-plane anisotropy of the AFM material and is of the order of  $10^8$  A/cm<sup>2</sup> for NiO AFM [19].

If the driving current is below the generation threshold, the AFM oscillator will not have enough energy to overcome the anisotropy, but the equilibrium orientation of the AFM sublattices will be moved towards the hard direction in the easy plane. With an additional impulse of current, the AFM magnetizations will surpass the anisotropy energy barrier and perform a single half-turn in the easy plane, which will cause a single spike of the spin-pumping voltage. This response of a sub-threshold AFM spin Hall oscillator is similar to the reaction of a biological neuron to an external stimulus [15]. The AFM neurons and their networks also have other properties that resemble biological neural systems, such as refraction and delayed response [16].

As it was shown in Ref. [19], the dynamics of an AFM neuron can be described by the in-plane angle  $\phi$  that the Neel vector of the AFM makes with the easy axis of the AFM. Under rather general assumptions, the angle  $\phi$  obeys the second-order dynamical equation,

$$\frac{1}{\omega_{ex}} \ddot{\phi} + \alpha \dot{\phi} + \frac{\omega_e}{2} \sin 2\phi = \sigma I, \quad (1)$$

where  $\omega_{ex} = 2\pi f_{ex}$  is the exchange frequency of the AFM,  $\alpha$  is the effective Gilbert damping constant,  $\omega_e = 2\pi f_e$  is the easy axis anisotropy frequency,  $\sigma$  is the spin-torque efficiency defined by Eq. (3) in Ref. [19],  $I$  is the driving electric current. Further details about the derivation of Eq. (1) can be found in [15], [19]. Note, that the spin-pumping signal produced by the AFM is proportional to the angular velocity of the sublattice rotation  $\dot{\phi}$ . Namely, the inverse spin Hall voltage produced by the AFM neuron can be found as

$$V = \beta \dot{\phi}, \quad (2)$$

where the efficiency  $\beta = 0.11 \times 10^{-15}$  V · s is defined by Eq. (2) in Ref. [16].

In this work, we study the dynamics of a network of interconnected AFM neurons. Each neuron is described by its own phase  $\phi_i$  and obeys an equation similar to Eq. (1) with additional terms describing synaptic connections between the neurons:

$$\frac{1}{\omega_{ex}} \ddot{\phi}_i + \alpha \dot{\phi}_i + \frac{\omega_e}{2} \sin 2\phi_i = \sigma I + \sum_{i \neq k} \kappa_{ik} \dot{\phi}_k. \quad (3)$$

Here,  $i$  and  $k$  are indices that represent the  $i$ -th and  $k$ -th neurons, and  $\kappa_{ik}$  represents a matrix of coupling coefficients. Note, that the coupling signal produced by the  $k$ -th neuron is proportional to  $\dot{\phi}_k$ , in agreement with Eq. (2).

The connections between the AFM neurons can be realized by several means, for example, by connecting them with copper bridges. The copper would be able to carry a spike of spin current from one neuron to the next, allowing the output of the first neuron to act as the input for the second. Copper bridges produce constant synaptic coupling, resulting in fixed connections  $\kappa_{ik}$  between neurons. However, it is necessary to be able to alter synaptic values when training a neural network. To create trainable synapses, a different, probably much more complicated,

approach to creating variable synapses would be needed. In this paper, which primarily focuses on investigating the dynamics of AFM *neurons*, we did not assume any particular physical model of a synapse. Instead, the simulated synapses are considered to be “ideal” such that they can be adjusted instantaneously and to any value.

There is a remarkable similarity between the equation describing the AFM neuron and that describing the dynamics of a physical pendulum; therefore, each term in Eq. (3) can be characterized by its mechanical analog. As a result, the coefficient of the first term on the left-hand side of Eq. (3) defines an effective mass, indicating that the AFM neuron possesses an effective inertia due to AFM exchange. This inertia results in a delay between a neuron receiving an input and the resulting output, an effect not found in conventional artificial neurons. When AFM neurons are linked together, such that the output of one neuron acts as the input of the next, the delay is dependent on the coupling strength  $\kappa_{ik}$  between the neurons. The delay caused by inertia decreases as the strength between neurons increases. Thus, the firing time of the neuron can be easily controlled. This means that the AFM neurons are well-suited for neuromorphic algorithms in which time encoding of neuron spikes is used.

One such time-encoding approach, namely, spike pattern association neuron (SPAN) [18], is studied in this paper. The architecture of an AFM neural network realizing the SPAN algorithm is shown in Fig. 1(a). It consists of one output “SPAN” neuron connected to many neurons of the input layer. In our simulations, the input layer consisted of 25 neurons and encoding input symbols drawn in a  $5 \times 5$  binary grid. We used several shapes of the input symbols shown in Fig. 1(b). A blackened pixel in the input symbol causes a spike in the corresponding input neuron, while a white pixel will have no spike. The SPAN neuron is trained to output a spike at a certain prescribed time if the input symbol matches the pattern to be recognized. To achieve this, synaptic connections between the input layer and the SPAN neuron are adjusted during the training, as explained below.

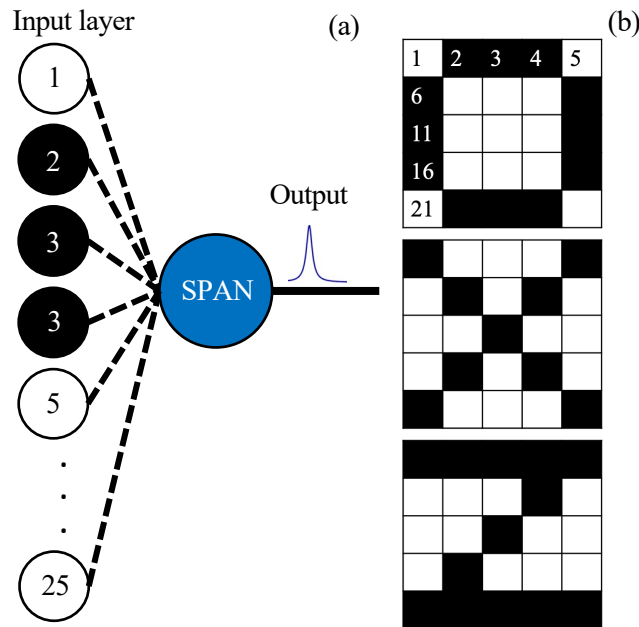


Figure 1. Single AFM SPAN neural network. (a) The architecture of AFM SPAN neural network. The input symbol is encoded in the spiking pattern of the input layer neurons. The synaptic weights between the input layer and the AFM SPAN neuron are adjusted during training. The temporal position of the SPAN's output spike encodes the outcome of pattern recognition. (b) Examples of the different input symbols used in pattern recognition where each pixel cell represents a different input neuron that will fire if the pixel is black.

We used parallel encoding of the input layer; namely, the input symbol triggers the input neurons to fire simultaneously. There will be an output spike if the combined weights connected to the SPAN are strong enough. The goal of training is to move this output spike to the desired time for a chosen symbol. If the spike is produced earlier (later) than the target time, the weights connected to the SPAN should reduce (increase).

In more detail, the SPAN training algorithm is based on the Widrow-Hoff rule, where the difference between the desired spike time  $t_d$  and the actual spike time  $t_a$  is used to update the synaptic weights. After some manipulation, shown in Ref. [20], the Widrow-Hoff rule is transformed to describe the change in weights during training:

$$\Delta\kappa = \lambda \left(\frac{e}{2}\right)^2 [(t_d - t_i + \tau)e^{-(t_d - t_i)/\tau} - (t_a - t_i + \tau)e^{-(t_a - t_i)/\tau}], \quad (4)$$

where  $\lambda$  is a positive and constant learning rate,  $t_i$  is the timing of the input spike,  $t_d$  is the desired timing of the output spike,  $t_a$  is the actual timing of the output spike, and  $\tau$  is a time constant corresponding to the width of a spike. Upon training, a SPAN should output its spike at the target time  $t_d$  for the correct symbol and spike away from the target time for any other symbol.

Figure 2 shows the output spikes of a SPAN neural network after training. When the correct symbol is supplied as input, the SPAN spikes within a 10 ps time window of the target time; this implies that the neural network has recognized chosen symbol. Any other symbol should cause a spike outside the target time window, indicating that a different symbol was used as input.

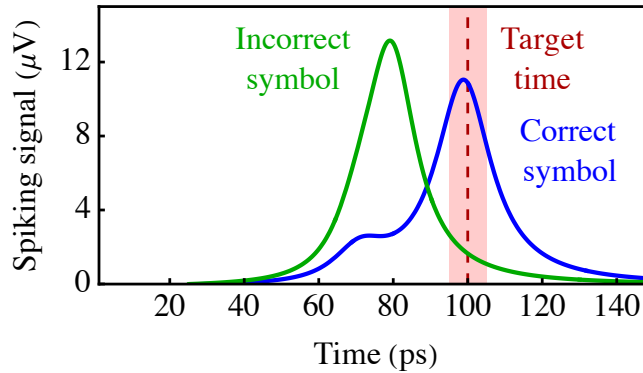


Figure 2: Simulation result of output signals generated by a trained AFM SPAN network. The red dashed line shows the target time for symbol recognition, with a 10 ps time window (red shading) encompassing the target time. The blue (green) line shows the simulated output spike of the AFM SPAN for the correct (incorrect) input symbol.

## Results and Discussion

A library of 20 symbols is used to train the neural network. These symbols are all variations of the correct symbol chosen from one of the symbols shown in Fig. 1(b). Variations include symbols with multiple additional or missing pixels. Initially initialized with random synaptic weights  $\kappa_{ik}$ , the neural network receives each symbol as an input during one training epoch. A symbol is associated with a target time corresponding to the image's difference from the correct symbol. Using this time and the actual timing of the output neuron, the SPAN algorithm determines how the weights should be changed in accordance with Eq. (4). The algorithm is modified to ensure that the weights cannot become negative, ensuring a more straightforward implementation in hardware. When all images have been processed, the weight changes resulting from each symbol are averaged, the neural network is updated, and the next epoch begins.

Figure 3(a) shows the error between the actual and desired spike time for the correct symbol throughout training, and Fig. 3(b) shows the corresponding changes in each synaptic weight. After an aggressive start, the change in weights is subtle for most of training. Due to the large number of inputs, each individual weight is relatively small, as only the total sum is relevant to the timing of the output spike. It should be noted that some weights continue to change throughout the whole of training. These weights, in particular, do not contribute significantly to any symbol in the training library and therefore have limited data when making weight adjustments.

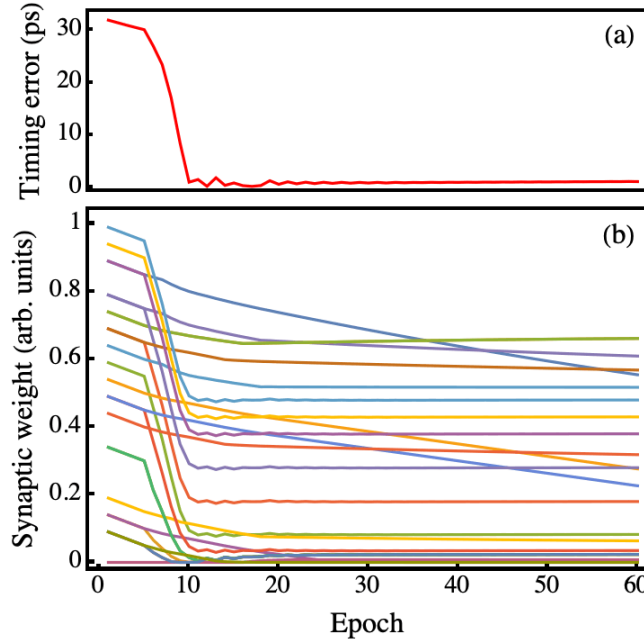


Figure 3: Simulations depicting the training process of an AFM SPAN. (a) Time difference between the target and actual spike times of the AFM SPAN's output over 60 epochs of training.

(b) Each colored line illustrates the evolution of an individual synaptic weight from an input neuron to the AFM SPAN over 60 epochs of training.

After about 10 epochs, the trained neural network will produce a spike within a 10ps widow of the target time when the symbol is recognized, as shown in Fig. 2.

Several examples of incorrect symbols serving as input and the resulting output spikes are shown in Fig. 4. By spiking outside the target time window for any symbol other than the correct symbol, the neural network has high accuracy in recognizing the chosen symbol. Whether additional or missing pixels serve as the difference from the correct image does not matter in making a spike outside of the target time window.

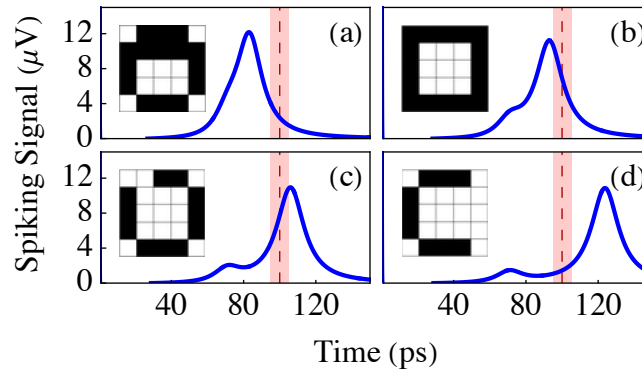


Figure 4: Simulation result of the output spikes of a trained AFM SPAN for different incorrect symbols, shown by insets. The dashed line represents the target time, and the red shading illustrates a 10 ps time window surrounding the target time. The simulated response for each incorrect symbol is outside the target time window, indicating that the inputted symbol is recognized to be *not* the correct symbol. (a, b) Input symbols have additional pixels. (c, d) Input symbols have missing pixels.

Multiple AFM SPANs, trained to recognize different symbols, can be connected to the same layer of input neurons. This way, the SPAN trained to the input symbol will produce a spike within the target time window, while the others would spike outside it. With multiple SPANs all spiking at different times, the output can be unclear. Therefore, it would be convenient to clear the output by suppressing output spikes outside the target time window. This can be done by creating an additional output layer that consists of fixed synapses, thus preserving the reservoir computing requirement that only synapses connecting the inputs to the SPAN layer are variable. The architecture of the neural network capable of suppressing unwanted outputs is shown in Fig. 5.



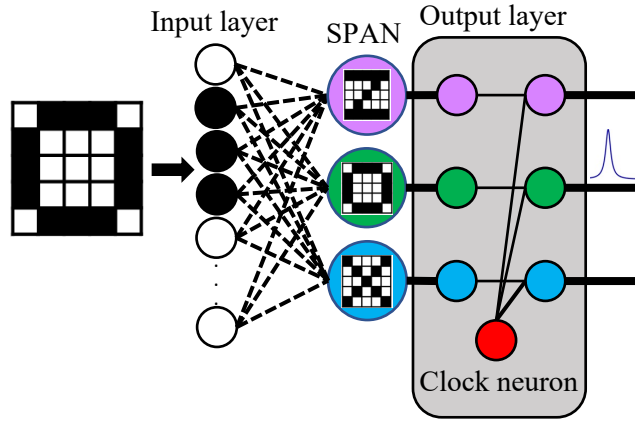


Figure 5: Architecture of a 3 AFM SPAN neural network. The input symbol is encoded in the spiking pattern of the input layer neurons. During training, the synaptic weights between the input neurons and each SPAN are adjusted individually as each SPAN is trained to recognize a different symbol. The weights of the output layer are weakened such that a single spike cannot propagate to the next neuron. The red neuron represents a clock neuron that spikes at the target time, combining with the SPAN corresponding to the recognized symbol to generate a sufficiently strong signal for the post-synaptic neuron to fire.

The input neurons are connected to three SPANs via trainable weights. These SPANs are each trained to recognize different symbols. The SPANs then serve as input to the output layer. The output layer's synapses have weak coupling, such that a single pre-synaptic spike is insufficient to cause a spike in the post-synaptic neuron. Two spikes must happen simultaneously to produce a strong enough signal for a post-synaptic spike.

The red neuron, shown in Fig. 5, is a clock neuron spiking at the target time. Therefore, when a symbol is recognized, the SPAN will spike along with the clock neuron at the target time. These two signals are enough to overcome the weak coupling and cause the post-synaptic neuron to fire. The spikes from the SPANs that do not correspond to the input symbol would spike away from the target time, thus not combining with the clock neuron to cause an output spike. This output layer ensures that only the spike from the SPAN corresponding to the correct symbol is outputted. The output spiking signals of this neural network are shown in Fig. 6.

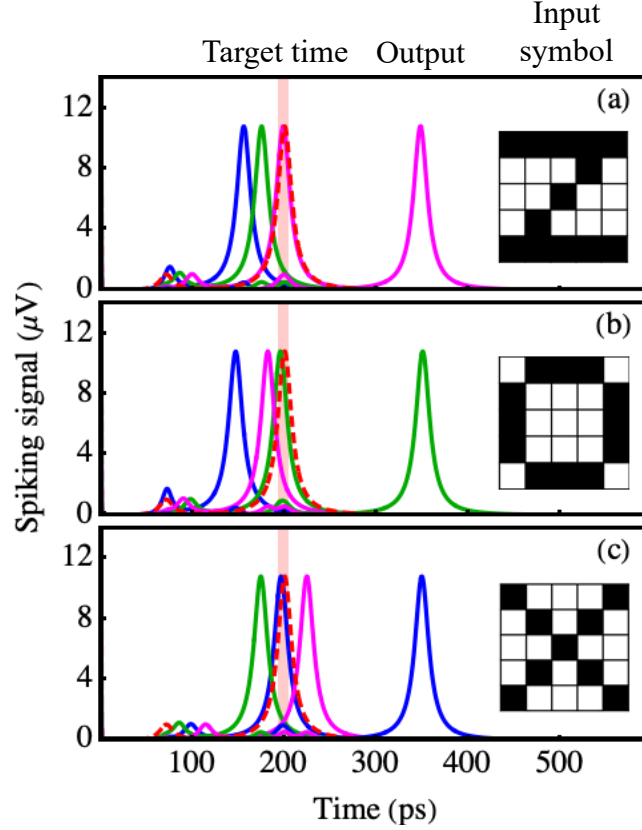


Figure 6: Simulated result of a 3 SPAN (pink, green, blue) neural network for 3 different input symbols (Z, O, X). The red shading represents a 10 ps time window surrounding the target time. The SPAN corresponding to the recognized symbol generates a spike within the target time window, along with the clock neuron (red dashed spike), resulting in a single output spike. The color of the output spike corresponds to the SPAN that was trained to recognize the inputted symbol.

The blue, green, and magenta spikes correspond to three different SPANs trained to three different symbols, while the red spike is the clock neuron spiking at the target time. At this time, there are the spikes of the clock neuron and a single SPAN corresponding to the inputted symbol. These two spikes combine to send a single spike to the output, indicating which symbol has been recognized. Therefore, this output layer creates an output that clearly identifies the recognized symbol.

## Conclusions

Ultra-fast spiking artificial neurons built from AFM oscillators have a number of unique properties that can be harnessed to create simple neural networks with fixed synapses [16]. However, in order to use AFM neurons in neuromorphic computing, a trainable neural network with variable synapses is required. The physical implementation of variable synapses is much more complex than fixed ones; therefore, in this work, we studied the application of ideas of reservoir computing, which limit the number of trainable weights and reduce the complexity of

the neural network. Namely, we numerically investigated the performance of the SPAN algorithm for the recognition of symbols encoded in a 5x5 binary grid.

The simulated AFM neural networks are capable of recognizing symbols by producing a spike within a target time window (10 ps). The training time of the AFM networks for such relatively small images is very short, about 10 epochs with a 20-symbol library. Due to the high speed of AFM neurons (200 ps between inputting a symbol and the output neuron firing), this training session may last for only ~40 ns of real-time.

Multiple SPANs, trained to different symbols, can be connected to the same inputs, thus providing multi-symbol recognition capabilities. With the addition of a fixed output layer suppressing spikes outside the target time window, the neural network will produce a single spike corresponding to the recognized symbol in just a few hundred picoseconds.

The energy consumption of a single AFM neuron, with dimensions described in Ref. [16], is about  $10^{-3}$  pJ per synaptic operation. In comparison, the energy per operation for the Intel Loihi Neuromorphic Chip was reported to be 20 pJ [1]. To successfully train a single SPAN, the total energy consumption of the AFM neural network is 31.2 pJ.

The use of reservoir computing and the SPAN algorithm leads to a very simple, one-layer neural network. This neural network is limited in its ability to perform more complex tasks as a result of such simplifications. For example, the MNIST data set of handwritten digits, commonly used for neural network training, is encoded in 28x28 pixel grids. It is unlikely that a neural network such as the one studied here would be able to cope with inputs on this scale. In order to advance the use of AFM neurons in neuromorphic computing, a more complex neural network and learning algorithm are required. However, even the simple network described in this work may find practical applications when high training, operation speed, and/or low consumed power are required.

## References

- [1] M. Davies *et al.*, “Loihi: A Neuromorphic Manycore Processor with On-Chip Learning,” *IEEE Micro*, vol. PP, pp. 1–1, Jan. 2018, doi: 10.1109/MM.2018.112130359.
- [2] J. Grollier, D. Querlioz, K. Y. Camsari, K. Everschor-Sitte, S. Fukami, and M. D. Stiles, “Neuromorphic spintronics,” *Nat. Electron.*, vol. 3, no. 7, Art. no. 7, Jul. 2020, doi: 10.1038/s41928-019-0360-9.
- [3] G. J. Lim, C. C. I. Ang, and W. S. Lew, “Spintronics for Neuromorphic Engineering,” in *Emerging Non-volatile Memory Technologies: Physics, Engineering, and Applications*, W. S. Lew, G. J. Lim, and P. A. Dananjaya, Eds., Singapore: Springer, 2021, pp. 297–315. doi: 10.1007/978-981-15-6912-8\_9.
- [4] N. Hassan *et al.*, “Magnetic domain wall neuron with lateral inhibition,” *J. Appl. Phys.*, vol. 124, no. 15, p. 152127, 2018.
- [5] W. H. Brigner *et al.*, “Shape-Based Magnetic Domain Wall Drift for an Artificial Spintronic Leaky Integrate-and-Fire Neuron,” *IEEE Trans. Electron Devices*, vol. 66, no. 11, pp. 4970–4975, Nov. 2019, doi: 10.1109/TED.2019.2938952.
- [6] D. Wang *et al.*, “Spintronic leaky-integrate-fire spiking neurons with self-reset and winner-takes-all for neuromorphic computing,” *Nat. Commun.*, vol. 14, no. 1, Art. no. 1, Feb. 2023, doi: 10.1038/s41467-023-36728-1.
- [7] “A tunable magnetic skyrmion neuron cluster for energy efficient artificial neural network | IEEE Conference Publication | IEEE Xplore.” <https://ieeexplore.ieee.org/abstract/document/7927015/> (accessed Apr. 05, 2023).
- [8] X. Chen *et al.*, “A compact skyrmionic leaky–integrate–fire spiking neuron device,” *Nanoscale*, vol. 10, no. 13, pp. 6139–6146, Mar. 2018, doi: 10.1039/C7NR09722K.
- [9] S. Li, W. Kang, Y. Huang, X. Zhang, Y. Zhou, and W. ZHAO, “Magnetic skyrmion-based artificial neuron device,” *Nanotechnology*, vol. 28, p. 31LT01, Jul. 2017, doi: 10.1088/1361-6528/aa7af5.
- [10] J. Torrejon *et al.*, “Neuromorphic computing with nanoscale spintronic oscillators,” *Nature*, vol. 547, no. 7664, Art. no. 7664, Jul. 2017, doi: 10.1038/nature23011.
- [11] A. Sengupta, P. Panda, P. Wijesinghe, Y. Kim, and K. Roy, “Magnetic Tunnel Junction Mimics Stochastic Cortical Spiking Neurons,” *Sci. Rep.*, vol. 6, no. 1, Art. no. 1, Jul. 2016, doi: 10.1038/srep30039.
- [12] M. Zahedinejad *et al.*, “Two-dimensional mutually synchronized spin Hall nano-oscillator arrays for neuromorphic computing,” *Nat. Nanotechnol.*, vol. 15, no. 1, Art. no. 1, Jan. 2020, doi: 10.1038/s41565-019-0593-9.
- [13] J. Cai *et al.*, “Voltage-Controlled Spintronic Stochastic Neuron Based on a Magnetic Tunnel Junction,” *Phys. Rev. Appl.*, vol. 11, no. 3, p. 034015, Mar. 2019, doi: 10.1103/PhysRevApplied.11.034015.
- [14] D. R. Rodrigues *et al.*, “A spintronic Huxley-Hodgkin-analogue neuron implemented with a single magnetic tunnel junction.” arXiv, Apr. 13, 2023. Accessed: Jun. 23, 2023. [Online]. Available: <http://arxiv.org/abs/2304.06343>
- [15] R. Khymyn *et al.*, “Ultra-fast artificial neuron: generation of picosecond-duration spikes in a current-driven antiferromagnetic auto-oscillator,” *Sci. Rep.*, vol. 8, no. 1, Art. no. 1, Oct. 2018, doi: 10.1038/s41598-018-33697-0.

- [16] H. Bradley *et al.*, “Artificial neurons based on antiferromagnetic auto-oscillators as a platform for neuromorphic computing,” *AIP Adv.*, vol. 13, no. 1, p. 015206, Jan. 2023, doi: 10.1063/5.0128530.
- [17] G. Tanaka *et al.*, “Recent advances in physical reservoir computing: A review,” *Neural Netw.*, vol. 115, pp. 100–123, Jul. 2019, doi: 10.1016/j.neunet.2019.03.005.
- [18] A. Mohemmed, S. Schliebs, S. Matsuda, and N. Kasabov, “Method for Training a Spiking Neuron to Associate Input-Output Spike Trains,” in *Engineering Applications of Neural Networks*, L. Iliadis and C. Jayne, Eds., in IFIP Advances in Information and Communication Technology. Berlin, Heidelberg: Springer, 2011, pp. 219–228. doi: 10.1007/978-3-642-23957-1\_25.
- [19] R. Khymyn, I. Lisenkov, V. Tiberkevich, B. A. Ivanov, and A. Slavin, “Antiferromagnetic THz-frequency Josephson-like Oscillator Driven by Spin Current,” *Sci. Rep.*, vol. 7, no. 1, Art. no. 1, Mar. 2017, doi: 10.1038/srep43705.
- [20] A. Mohemmed, S. Schliebs, S. Matsuda, and N. Kasabov, “Training spiking neural networks to associate spatio-temporal input–output spike patterns,” *Neurocomputing*, vol. 107, pp. 3–10, May 2013, doi: 10.1016/j.neucom.2012.08.034.